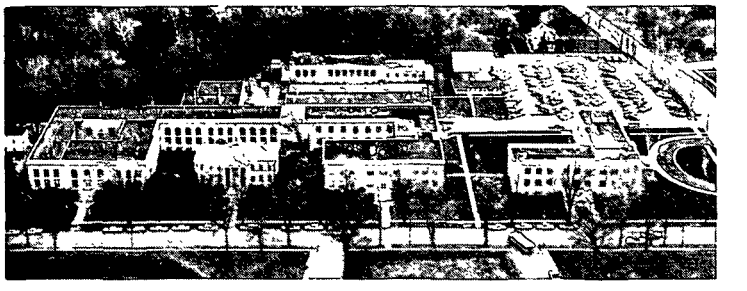

THE INSTITUTE OF PAPER CHEMISTRY, APPLETON, WISCONSIN

IPC TECHNICAL PAPER SERIES
NUMBER 48

THE MEASUREMENT OF OPTICAL UNEVENNESS

R. M. LEEKLEY, R. F. TYLER, AND J. D. HULTMAN

JANUARY, 1978

THE MEASUREMENT OF OPTICAL UNEVENNESS

R. M. Leekley, R. F. Tyler and J. D. Hultman

ABSTRACT

The quality of printing papers is known to be an important factor in the visual "roughness" or optical unevenness which is frequently the basis for printing complaints. Even though the ultimate evaluation of this characteristic must be subjective, an instrumental method for predicting whether a printed product will be judged to be objectionally uneven would be useful to the paper-maker for evaluation of test prints. An instrument which compares the reflectance of small spot areas along a scanning path with the simultaneously sensed average reflectance of the surrounding area has been developed. Numerous statistical descriptions of the scanning data have been compared with subjective evaluations to determine the most satisfactory unevenness number. An instrument is now being developed to provide digital readout of the preferred unevenness number.

This paper has been submitted for publication in Tappi.

THE MEASUREMENT OF OPTICAL UNEVENNESS

R. M. Leekley, R. F. Tyler and J. D. Hultman

INTRODUCTION

The quality of printing paper is known to be an important factor in the visual "roughness" or optical unevenness which is frequently the basis for printing complaints. The printed product is intended for visual appreciation so it is the subjective evaluation of the print which is of real importance. However, instrumental methods of predicting whether a printed product will be judged to be objectionably uneven would be useful to the papermaker for evaluation of test prints.

There are several problems in designing an instrumental method of predicting visual unevenness. One is in choosing the type of variation the instrument should sense. This involves the incident and receptor angles, the aperture size, the spectral distribution, etc. Another problem involves the statistical description of the data as an unevenness number which will correlate with visual assessment. Finally it is necessary to have a method of visual evaluation which will provide numerical subjective data against which the instrumental unevenness numbers can be evaluated.

DESIGN OF THE INSTRUMENT

The basic feature of simultaneous detection and comparison of the small spot reflectance with the larger surrounding area, which was employed previously (1), has been retained. The optical system is shown schematically in Fig. 1. The principal change required was the replacement of the photoconductive receptors which, because of their "memory," severely limited the scanning speed of the original instrument. Change to silicon photodiodes required other changes in electrical circuitry and in level of illumination.

[Fig. 1 here]

Two silicon photodioides (United Detector Technology PIN 10) are used to detect the light transmitted through the small and large apertures of the instrument. Signals from these cells are amplified in the two channel solid state amplifier shown in the schematic diagram of Fig. 2. One of the amplified signals is then inverted in polarity and mixed with the other signal to provide a difference signal which is further amplified. The output is a voltage which is proportional to the difference between the reflectances detected through the small and large apertures. In this respect it differs from the previously described instrument which provided the ratio of these reflectances. The reflectance of either the small spot or the large spot can be recorded by switching off the other channel.

[Fig. 2 here]

Incident light is provided by the optical system shown schematically in Fig. 3. The entire filament of a Sylvania BCL Tungsten-Halogen 300 watt projection lamp is focused by the condensing lens L_1 on the end of a 9 mm solid glass rod which is aluminized on its cylindrical surface. Light issuing from the other end of the glass rod is focussed upon the specimen by the lens L_2. This permits utilization of substantially all of the light entering the rod from the whole filament to illuminate a restricted area of the specimen without having the image of the filament in focus at the specimen. It should be noted that the light is not collimated. The beam issuing from lens L_2 has a bullseye pattern due to portions of the light which are subject to 0, 1, 2, etc., reflections within the rod. However, this pattern converges to form a uniform image of the exit end of the rod upon the specimen. There appears to be no disadvantage to using noncollimated light and there may be some advantage in that the effect of surface roughness upon the detected profiles is probably reduced. The lamp is operated at 108 volts ac using a voltage regulator. This extends the life of the lamp considerably beyond the 1000 hours for which it is rated at 120 volts ac. The lamp house is cooled with a fan and in addition there

is a 1/4 inch tempered heat absorbing glass plate between the lamp and the condensing lens.

[Fig. 3 here]

The maximum sensitivity of the silicon photodiodes is in the near infrared region. Therefore, filters are required in the light source to convert the overall instrument response to that of the eye, i.e., the CIE $\bar{y}$ function. These filters are inserted in the light path at the exit end of the glass rod. The method of Van den Akker and Dearth (2) for calibration of filter colorimeters was used to select the proper combination of filters. Because of the spectral distribution chosen the reflectances through the small and large apertures and their difference are designated as Y_S, Y_L and $Y_S - Y_L$, respectively.

As illustrated in Fig. 1 the instrument employs 45-0° viewing geometry. With this geometry the specular component of reflected light is excluded so that the unevenness detected is due to uneven absorption or transmission of light by the specimen. Gloss mottle contributes very little to the unevenness measured at this viewing condition. The additional optional 0-0° viewing condition which is illustrated schematically in Fig. 4 has also been provided. The method is that previously used by Leekley and Tyler (1). At 0-0° viewing geometry the specular component of reflected light is included so the instrument is sensitive to gloss mottle.

[Fig. 4 here]

The shape of the small aperture is not critical for scanning unprinted papers or solid prints. However a square aperture has an advantage where syzygetic* scanning is desired because the whole sample can be covered without overlap or missing any sample area. However the shape is of greater importance for scanning

*The term syzygetic indicates that values are determined for each adjacent aperture area.

halftone prints because of the need to suppress the pattern of the dots. Diehl (3) was apparently first to report a scanning device to measure the integrated reflectance from the unit cell of a halftone print. This requires a square aperture the exact size of the unit cell which is precisely oriented with the screen direction. The scanning direction is unimportant. Nordman and Makkonen (4) have also used square apertures to scan halftones. It is, of course, possible to use larger square apertures. A square with side n times the screen ruling distance will include a constant integrated dot area equivalent to 1, 4, 9, ... n^2 individual dots. It is also possible to use a square oriented along the diagonal of the screen pattern. In this case a square m times the diagonal distance will include a constant integrated dot area equivalent to 2, 8, 18, ... $2m^2$ individual dots. Use of the larger apertures increases the requirement for sensitivity because the effect of a small improperly printed area is integrated over a larger area.

The instrument is provided with a square small aperture which can be adjusted in size to conform to the screen ruling of the print being tested. This square opening is formed between two V-leaves as illustrated in Fig. 5. The size of the square is changed by adjustment of micrometers which control the position of the leaves. Due to magnification, the actual specimen area imaged on the aperture is approximately 1/5 the actual size of the aperture. Therefore it was necessary to relate the micrometer scales to the effective aperture in the specimen plane. A 150 line/inch Ronchi ruling was placed at the specimen plane with its lines at right angle to the scanning direction. The aperture was oriented with sides parallel and perpendicular to the lines of the ruling. Scans were made at varying micrometer settings. The instrument is unable to detect the lines of the ruling when the side of the square effective aperture is exactly 1, 2, 3 ... n line pairs but produces a signal of increasing amplitude as the effective aperture approaches 1/2, 1-1/2, 2-1/2 ... n-1/2 line pairs. The micrometer readings at which signals of minimum amplitude

were obtained were plotted against the distance established by the number of line pairs to provide the calibration chart. The settings for the two micrometers required to adjust to the appropriate effective aperture size are read from this plot. The combinations of micrometer settings keep the square centered regardless of size.

[Fig. 5 here]

The large aperture is round and approximately one-half inch in effective diameter. This size is an arbitrary choice which seems to be satisfactory. No work has been done on determining the optimum size for this aperture.

Calibration standards of excellent evenness are required to insure that the difference in reflectance between the small spot area and the average of the surrounding area is measured accurately. The Munsell* gray cards have been adopted as calibration standards at 45-0° viewing geometry. The Munsell standard closest in visual darkness to the sample to be measured is selected; and with only the large aperture amplifier turned on, the gain is adjusted to the proper luminous reflectance, Y, on a scale in which 10 volts corresponds to 100%. The small aperture amplifier is then also turned on and its gain adjusted to a luminous reflectance difference of zero.

The scanning mechanism is illustrated schematically in Fig. 6. A 3/8-inch thick aluminum plate carrying the specimen is pushed and pulled back and forth through the instrument by a lead screw which is driven by a reversible synchronous motor M_1. The length of travel is restricted to 3 inches by microswitches which turn off motor M_1 and turn on synchronous motor M_2. Motor M_2 is coupled by a lead screw to wedge W which moves the specimen holder laterally. The lateral distance the holder moves is controlled by an adjustable timer which governs the length of time

*Munsell Color, Macbeth Division of Kollmorgen Corporation, 2441 N. Calvert St., Baltimore, Maryland 21218.

M_2 is permitted to run. This interval is usually chosen to move the specimen the width of the area viewed through the small aperture. When the timer shuts off M_2 it turns on M_1 which reverses direction between scanning paths. It is therefore possible to scan the sample in a series of parallel adjacent but nonoverlapping paths.

[Fig. 6 here]

Sampling Signal

The instrument provides a continuous analog signal along each scanning path. It is necessary to sample this analog signal at uniform intervals. For syzygetic scanning this interval must correspond to the length of scanning path visible at one time through the small aperture. The cone and disk arrangement driven by motor M_1 provides a sampling signal. The rotating disk has two small magnets which momentarily close stationary reed switches to provide a pulsed signal from a battery. Two or four pulses per revolution of the disk are obtained depending on whether the output of one or both reed switches is accepted. The location of the disk on the cone provides an additional continuous adjustment in pulse frequency with respect to the motor M_1. Sampling pulses are generated only when motor M_1 is operating. Therefore with the pulsing frequency and the lateral movement both adjusted to correspond to the area viewed through the small square aperture, a pulse is generated when and only when a complete new specimen area comes into view through this aperture. Values of the analog signal sampled at these pulse intervals correspond to elemental areas of the size covered by the aperture without skipping or overlapping within the scanned area.

The data are logged in analog form on magnetic tape using a Hewlett-Packard 3960 instrumentation tape recorder with 2 FM and 2 AM channels. Channel 1 (FM) is used for recording the analog signal and Channel 2 (FM) for the pulsing sampling signal. In addition Channel 1 is used to record a digital sample code prior to scanning. An ac signal is recorded on Channel 3 (AM) during collection of data and

is turned off to signal the end of scanning. All data is logged at a tape speed of 15/16 inch/second.

The primary data recorded is $\underline{Y}_S - \underline{Y}_L$, the difference between the reflectance of small areas sensed through the small aperture and the average reflectance of the surrounding area. However it is desirable to be able to calculate the actual reflectance of the small areas. Therefore the practice of first recording the local average reflectance sensed through the large aperture by scanning a single path along the central part of the test strip was adopted. The reflectance difference, $\underline{Y}_S - \underline{Y}_L$, is then recorded for multiple parallel scanning paths. This permitted calculation of $\underline{Y}_S$ by adding a $\underline{Y}_L$ value representative of the proper longitudinal location on the test specimen. The data were digitized with a PDP 11/20 Laboratory computer system running a program written in the LABASIC language which is capable of providing 2^{10} (1024) digital values of both negative and positive numbers. The digitizer was programmed to sample the analog signal and record its digital value when the pulsing signal exceeds a threshold level. No additional sampling occurs until the pulsing signal diminishes and again rises to exceed this threshold. The digital values for one scanning line are recorded in the instrument memory (limit 256 values) and are transcribed to magnetic tape during the gap in pulses occurring between scanning lines. The analog tape is digitized at a speed of 15 inches/second or 16 times the speed at which it is recorded. The digital magnetic tape is then edited in form suitable for further calculations on the IPC computer. This among other things involves the calculation of $\underline{Y}_S$ values. Since the direction of scan changes between adjacent scanning paths for $\underline{Y}_S - \underline{Y}_L$ and $\underline{Y}_L$ is determined by scanning in only one direction, an inversion in order of $\underline{Y}_L$ values is made in calculating $\underline{Y}_S$ for even numbered scanning paths.

STATISTICAL DESCRIPTION OF UNEVENNESS

Although previous workers (5) have employed a variety of statistical descriptions of unevenness data, little experimental evidence has been reported which would establish the comparative suitability of the different statistics for measuring visually detectable unevenness. The availability of the present data in digital form on magnetic tape makes it possible for the first time to compare a wide variety of statistical descriptions for suitability as unevenness numbers.

In the past unevenness has been expressed as the standard deviation of reflectance, σ_R; the coefficient of variation of reflectance, $\sigma_R/\bar{R}$, where R is the average reflectance; the standard deviation in reflection density σ_D; or the average syzygetic density difference. Nordman and Makkonen (4) prefer the product of the coefficient of variation of reflectance and the logarithm of the average reflectance, $\sigma_R/\bar{R} \cdot \log \bar{R}$; which they say is suitable for comparing samples even when they are different in average darkness. One might expect that a statistic based on a visually uniform lightness scale, such as the Munsell value, V, or the Wyszecki (6) lightness, W, would be suitable for comparing the unevenness of samples of varying average darkness.

The following quantities have been calculated for all data points:

The luminous reflectance difference $Y_S - Y_L$ supplied directly by the instrument.

The luminous reflectance of the small aperture areas Y_S which is calculated by addition of Y_L to $Y_S - Y_L$.

The Munsell value of small aperture areas, V_S, which is approximated by the equation of Voglesong (7).

$$V_S = -1.32 + 2.2\, Y_S^{0.352}$$

The lightness of the small aperture areas W_S which is given by the equation of Wyszecki (6).

$$W_S = 25\ Y^{1/3} - 17$$

The reflection density difference between small and large aperture areas was calculated from Y_S-Y_L and Y_L as indicated by the equations:

$$\Delta D_{L-S} = \log \frac{1}{Y_L} - \log \frac{1}{Y_S} = \log \frac{Y_S}{Y_L} = \log \frac{Y_S - Y_L}{Y_L} + 1$$

The absolute value* of the syzygetic density difference, which is the difference in reflection density between adjacent small aperture areas expressed as a positive number,

$$|S\Delta D| = \left| \log \frac{1}{Y_{S(n)}} - \log \frac{1}{Y_{S(n+1)}} \right| = \left| \log \frac{Y_{S(n+1)}}{Y_{S(n)}} \right|$$

Averages, standard deviations, coefficient of variations and the product of coefficient of variation and the logarithm of average were computed for all of these variables. The use of the last statistic (product of coefficient of variation and the log of the average) followed the Makkonen and Nordman (4) treatment of reflectance measurements and has been arbitrarily extended to the other variables.

METHOD OF SUBJECTIVE EVALUATION

Pair comparison is probably the most used method of subjective evaluation within the Graphic Arts Industry. However this technique provides only an ordinal rank. It would be preferable to have a cardinal scale so that regression and correlation coefficients with the objective values could be used. Furthermore the examination

* It is necessary to use the absolute value because if the sign is retained all except the first and last data points would appear in both positive and negative form when the average is computed.

of samples by pairs provides the judge with opportunity to change his judging criteria during the experiment. A circular result that A>B, B>C and C>A may not mean that the samples are indistinguishable. It could mean that the samples differ in different respects and that the judge has changed his judging criteria in response to the changing type of difference present as different pairs were judged. For these reasons pair comparison was rejected and a method of developing a ratio scale, fashioned after that described by Woodworth and Schlosberg (8) was adopted.

The set of 4 to 15 samples is displayed all at once in random order on the viewing table and the judge is instructed to first arrange the samples in order of decreasing quality as determined by evenness of tone. A score of 10 is arbitrarily assigned to the poorest sample. Then, working up the quality scale, higher and higher scores are assigned in turn such that the relative scores of adjacent samples seem appropraite to their relative evenness. Composite scores for the individual samples are obtained by calculating the geometric mean of the scores provided by the individual judges. This is done conveniently by averaging the logarithms of the individual judges scores to provide the logarithm of the composite score. It should be noted that this is a subjective evenness number which increases with increasing evenness. It is the logarithm of the subjective evenness, S, which has been useful in correlation with the objective unevenness statistics.

The type of unevenness visible during subjective evenness evaluations is strongly dependent on the viewing geometry. Most of the work has been done at 45°-0° viewing geometry and comparison is made to objective data made at the same geometry. For gloss mottle the observation is made at glare angle of about 30°-30° although the objective measurement is at 0°-0°.

DISCUSSION OF RESULTS

A large number of prints were made with black ink on a variety of papers using the Vandercook proof press. Two plates, both of 120 lines per inch, one with approximately 20% printing area and the other with about 50% printing area, were used. Impression was varied to give a large population of prints which differed widely in visual evenness. From these a set of 10 light prints (20% printing area) and a set of 12 dark prints (50% printing area) were selected. Each set was subjectively graded for evenness. Each of the prints were scanned with both 2 dot and 8 dot small apertures and correlation coefficients of objective unevenness statistics with the logarithms of subjective evenness values were calculated for both sets. These correlation coefficients for the eight most promising statistics are shown in columns 2-5 of Table I. Next 7 samples were selected from each set to form a new closely spaced set of 14 mixed light and dark samples. This mixed set was subjectively graded for evenness, and correlation coefficients with these new values were calculated. These coefficients are shown in columns 6 and 7 of Table I.

[Table I here]

It is evident that $\sigma Y_S - Y_L$ provides the best correlation with subjective values in all cases. It is also noteworthy that the two statistics based on visually linear scales, σV_S and σW_S and the Nordman and Makkonen unevenness number, $\sigma Y_S \log Y_S/\bar{Y}_S$, in which the visually nonlinear Y scale is corrected by the factor $\log \bar{Y}_S/\bar{Y}_S$, provide nearly identical correlation coefficients. However they are inferior to $\sigma Y_S - Y_L$ in all cases and inferior to all of the other statistics listed in Table I for the set of mixed light and dark samples. The manner that average sample darkness affects σV_S and $\sigma Y_S \log \bar{Y}_S/\bar{Y}_S$ is illustrated in Fig. 7. It is evident that the Nordman and Makkonen unevenness number is substantially equivalent to σV_S but that both fail to correlate with visual assessments of unevenness where samples vary in average darkness.

In contrast $\sigma Y_S - Y_L$ which is illustrated in Fig. 8 does properly predict the visual unevenness of the same sample set.

[Fig. 7-8 here]

The values of Y_S used to calculate σY_S were, of course, calculated from $Y_S - Y_L$, which is the direct output of the instrument by addition of the appropriate Y_L values. It was of interest to determine how σY_S would differ if it were determined directly with a sample aperture instrument. This correlation is achieved by switching off the large aperture amplifier of the present instrument. The last two columns of Table I contain correlation coefficients for σY_S and the other statistics which can be calculated from Y_S for scans made under this single aperture condition on the set of 14 mixed samples. It is evident that none of these statistics provide the correlation with subjective values provided by $\sigma Y_S - Y_L$.

Comparisons have also been made between the same objective unevenness statistics and subjective evenness data for other letterpress halftone prints for solid letterpress prints on coated paper at both 45°-0° and 0°-0° viewing geometry, and for gravure prints. In all cases the correlation for $\sigma Y_S - Y_L$ was as high or higher than that for any of the other statistics. In none of these cases did any of the statistics based on visually uniform scales show any advantage.

The reason that the standard deviations of Munsell value and of Wyszecki unevenness number failed to properly predict visual evenness of samples which vary in average darkness is not known. It was for such sets of samples that these statistics were included. It may be that the psychophysical detection of unevenness does not depend upon the scale which has been established for the aesthetic assignment of equal lightness difference among large patches of differing but uniform lightness. It was not anticipated that $\sigma Y_S - Y_L$, which is based upon a scale known to be visually nonlinear,

would give satisfactory results even with sets of mixed darkness. The result is, however, fortunate because an instrument which will read directly in $\sigma Y_S - Y_L$ will be much easier to develop than one which utilizes a visually uniform scale. This development is now in progress.

LITERATURE CITED

1. Leekley, R. M. and Tyler, R. F., TAPPI 6th Graphic Arts Conference Preprints 1969:41-3. Tappi 58(3):124-7(1975).

2. Dearth, L. R., personal communication, 1975.

3. Diehl, H., Int. Bull. for Printing and Allied Trades 80:20-4(1958).

4. Makkonen, T. and Nordman, L., Paper and Timber 50:509-16(1968). Nordman, L. and Makkonen, T., Proceedings of the Tenth International Conference of Printing Research Institutes (Krems, Austria) 1969:271-82, Pergamon Press, 1971.

5. Karttunen, S. The influence of paper and printing conditions upon the unevenness of prints. Thesis, 1968, The State Institute for Technical Research, Finland.

6. Wyszecki, G. and Wright, H., J. Opt. Soc. Am. 55:1166(1965).

7. Voglesong, W. F. Image Technology, Feb./March, 1973:29.

8. Woodworth and Schlosberg, Experimental Psychology, Holt, Rinehart and Winston Inc. pp. 73-79.

TABLE I

CORRELATION COEFFICIENTS OF SELECTED OBJECTIVE UNEVENNESS STATISTICS WITH LOGARITHMS OF SUBJECTIVE EVENNESS

Statistic	10 Light[a] Samples		12 Dark[b] Samples		14 Mixed[c] Samples		14 Mixed Samples	
	2 Dot	8 Dot	2 Dot	8 Dot	2 Dot	8 Dot	2 Dot[d]	8 Dot[d]
σV_S	-0.82	-0.89	-0.90	-0.81	-0.34	-0.24	-0.26	-0.25
σW_S	-0.82	-0.89	-0.89	-0.81	-0.33	-0.23	-0.25	-0.25
$\sigma Y_S \log \bar{Y}_S/\bar{Y}_S$	-0.83	-0.88	-0.88	-0.80	-0.32	-0.22	-0.24	-0.24
σY_S	-0.78	-0.92	-0.97	-0.94	-0.71	-0.57	-0.75	-0.63
$\sigma Y_S - Y_L$	-0.97	-0.97	-0.98	-0.98	-0.98	-0.97	--	--
$\sigma D_L - D_S$	-0.95	-0.95	-0.92	-0.93	-0.52	-0.52	--	--
$\lvert S\Delta D \rvert$	-0.91	-0.89	-0.86	-0.86	-0.45	-0.44	-0.34	-0.26
$\sigma \lvert S\Delta D \rvert$	-0.96	-0.94	-0.86	-0.89	-0.60	-0.55	-0.91	-0.19

[a] Letterpress 120 line/inch halftone of 20% printing area.
[b] Letterpress 120 line/inch halftone of 50% printing area.
[c] 7 Light and 7 dark samples selected from the previous sets.
[d] Scanned using only the small aperture.

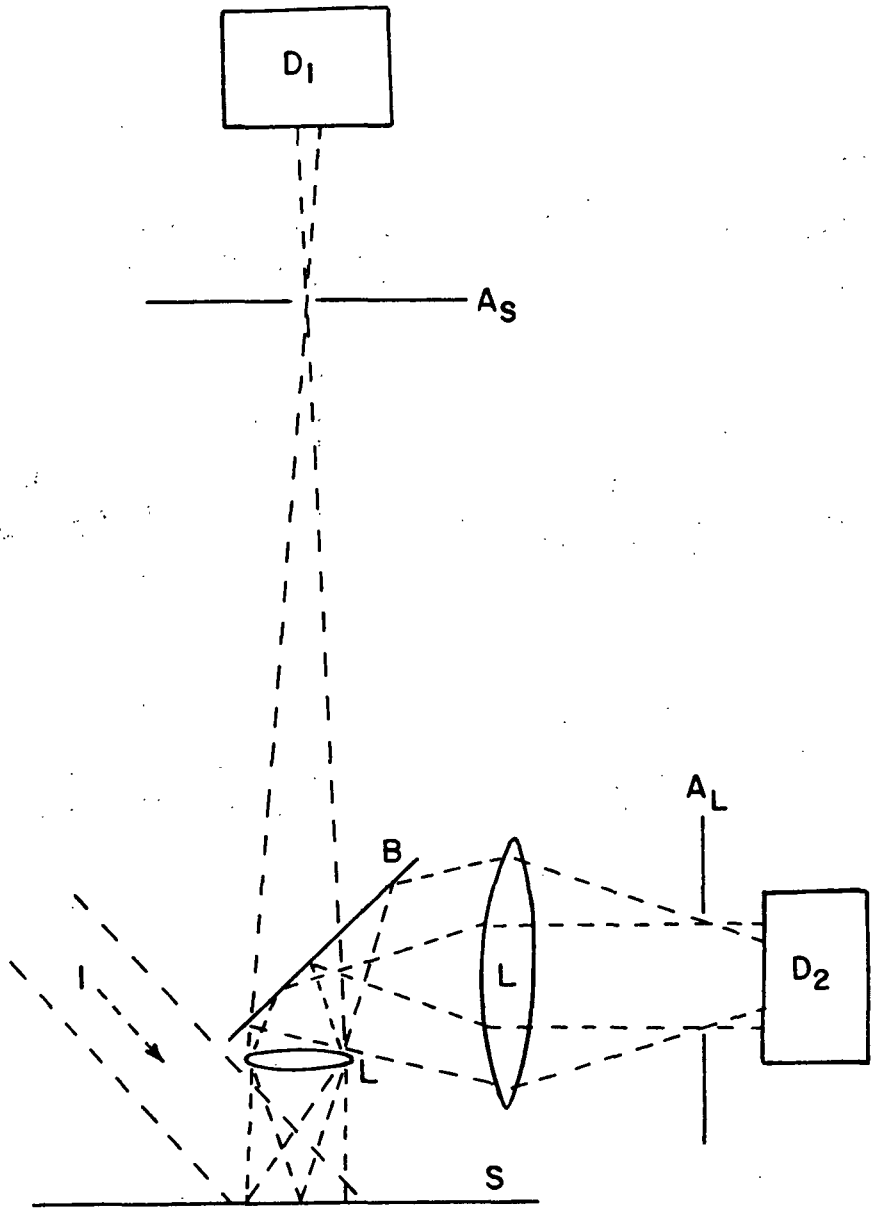

Figure 1. Schematic Diagram of the Optical System. I is the Incident Light Beam. Light Reflected by the Specimen, S, Passes Through the Lens, L, to the Clear Glass Beam Splitter, B. Light Transmitted by the Beam Splitter Which is Accepted by the Small Aperture, A_S, is Detected by the Photoreceptor, D_1. Light Reflected by the Beam Splitter and Accepted by the Large Aperture, A_L, is Detected by the Photoreceptor, D_2.

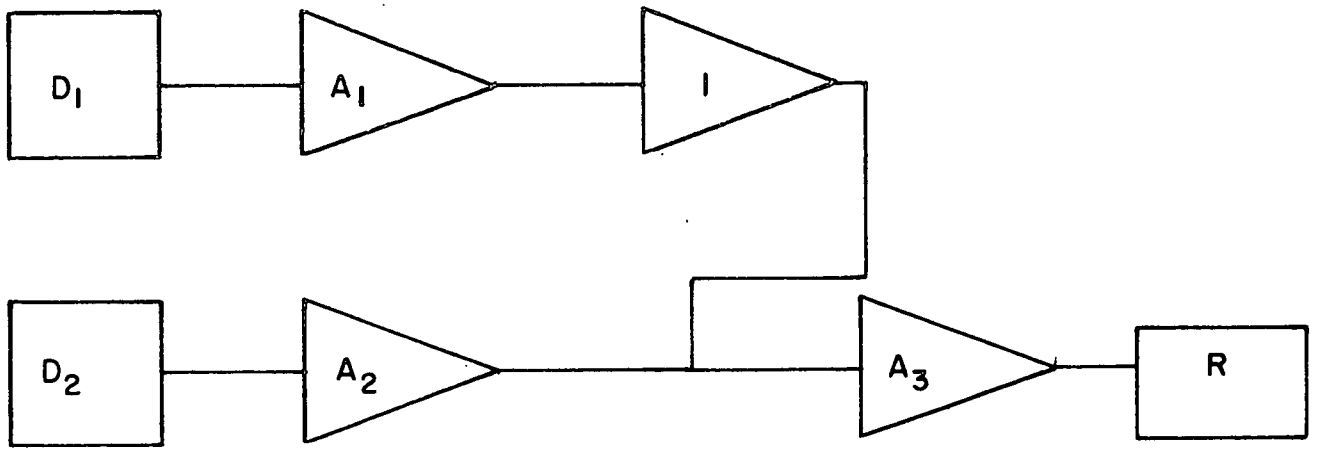

Figure 2. Schematic Diagram of the Amplifier System. D_1 and D_2 are the Detectors, A_1 and A_2 are the Amplifiers, I is the Signal Inverter, A_3 is the Difference Amplifier, and R is the Recorder.

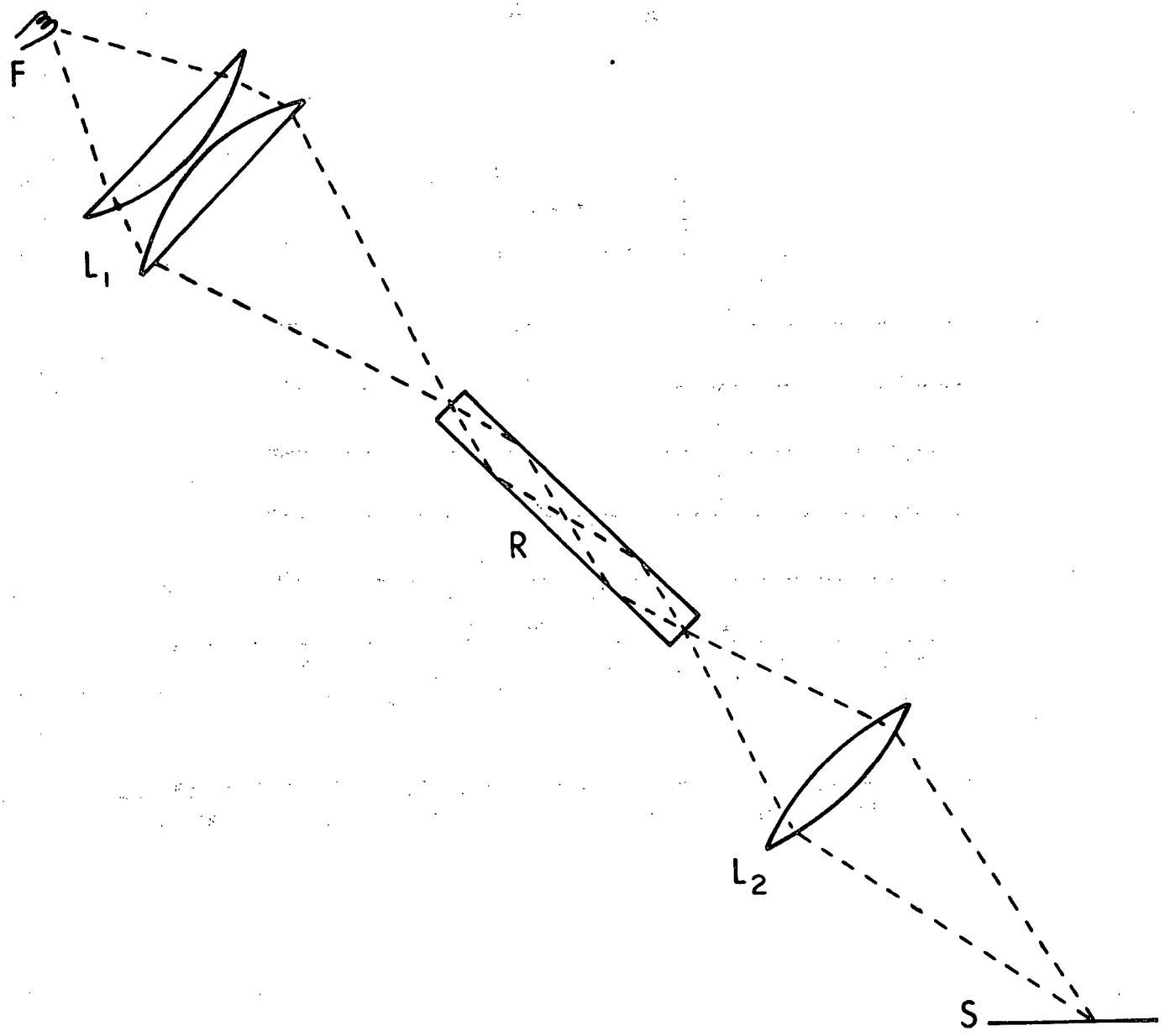

Figure 3. Schematic Diagram of the Incident Light Source. F is the Lamp Filament, L_1 and L_2 are Lenses, R is a Glass Rod Light Guide, and S is the Specimen.

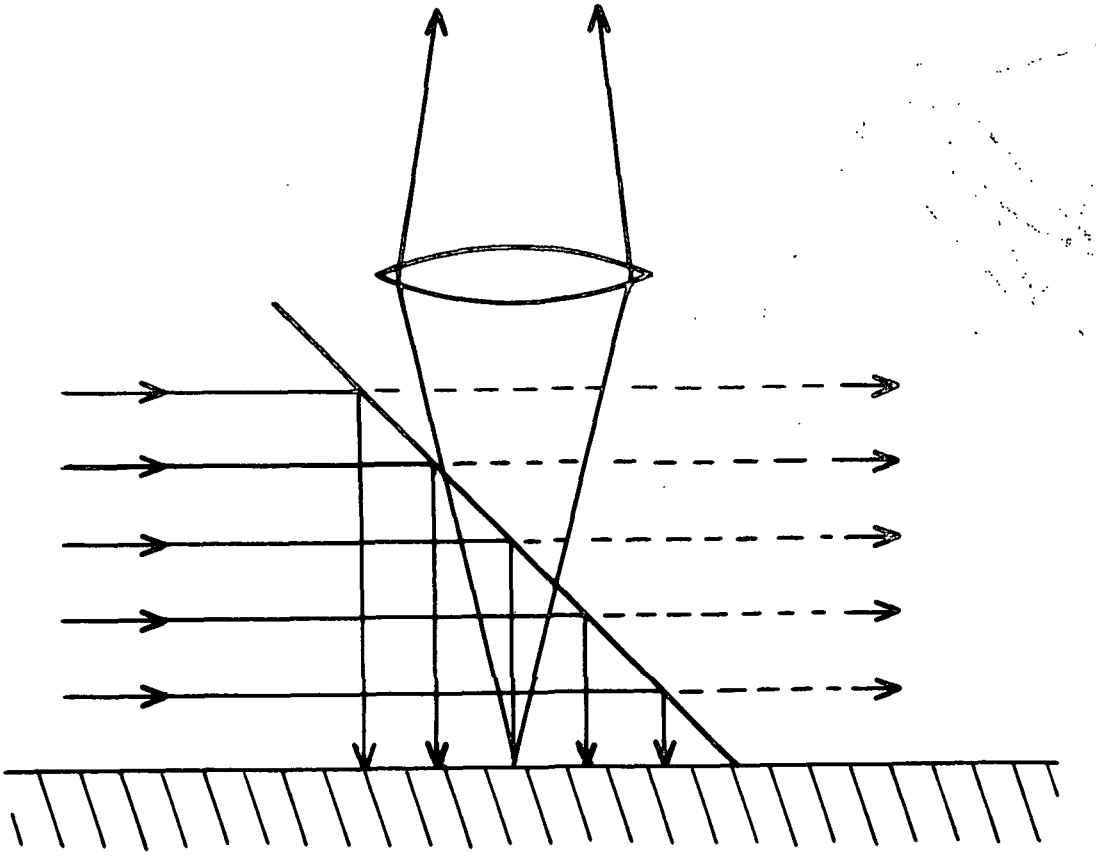

Figure 4. Schematic Diagram Showing the Inclined Partially Silvered Mirror Used to Achieve 0° Incidence for 0-0° Scanning.

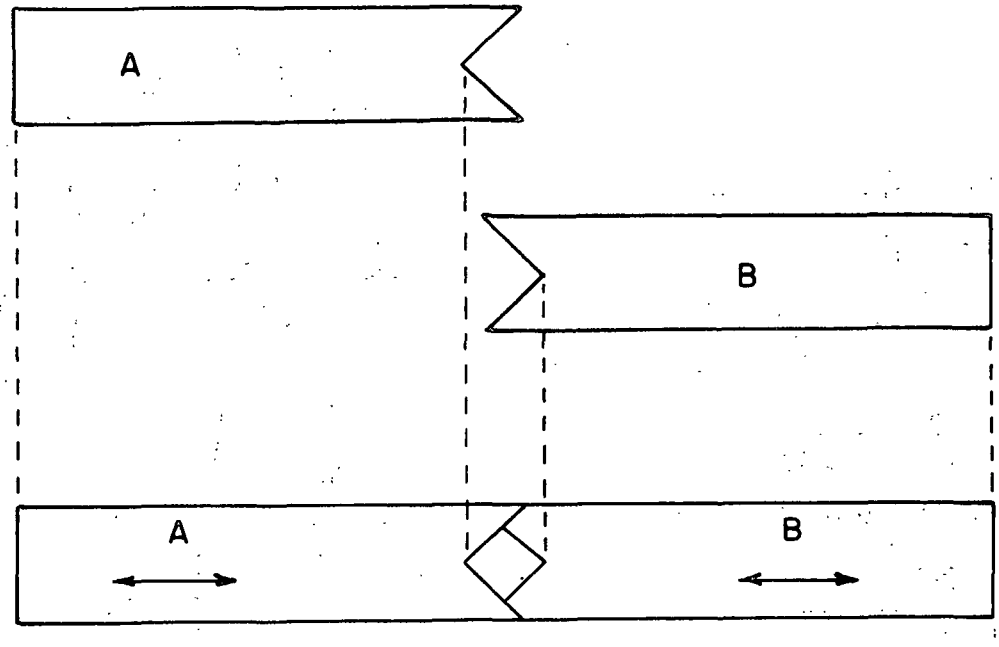

Figure 5. Schematic Diagram Showing How the Two Leaves A and B Overlap to Form a Square Aperture of Variable Size

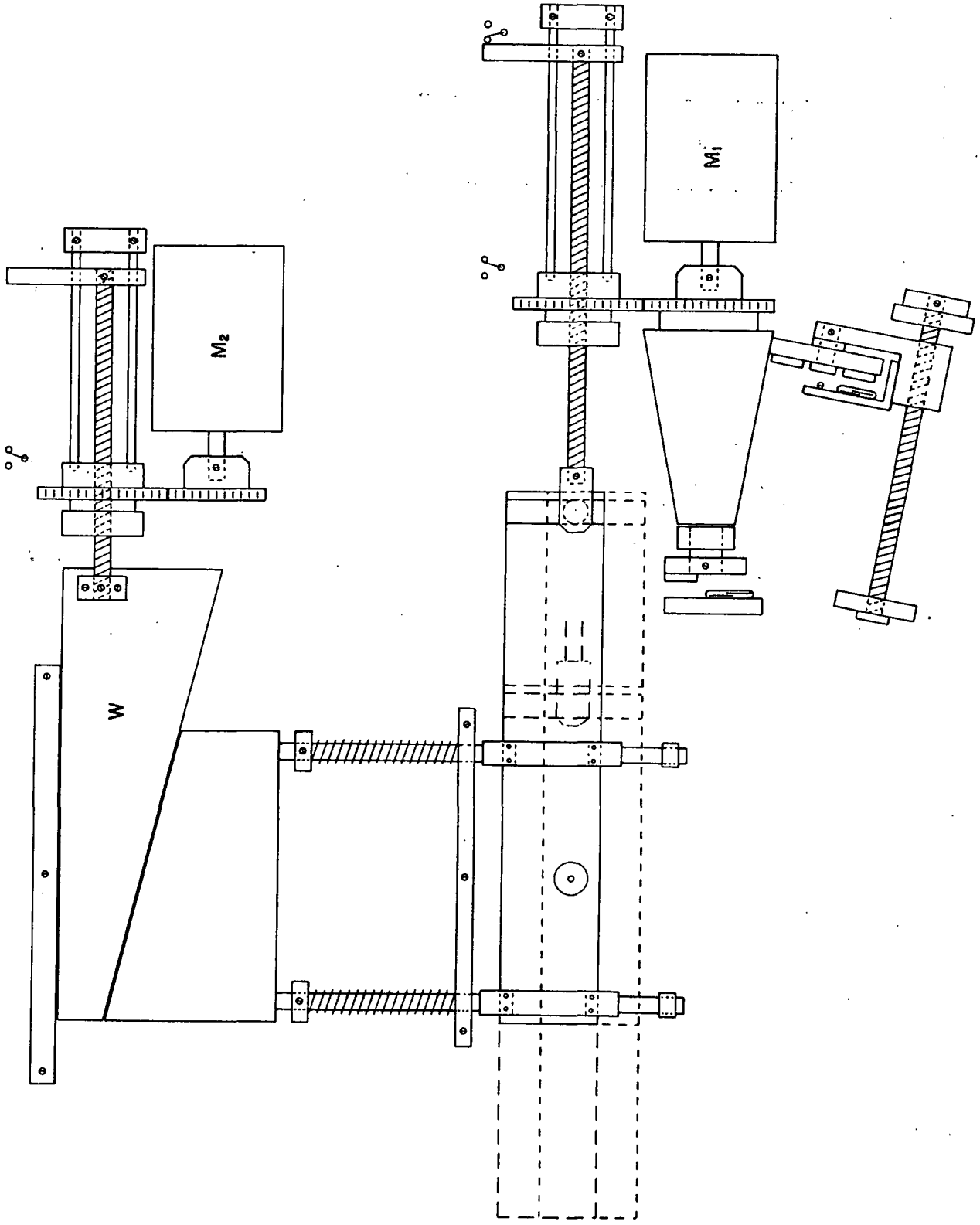

Figure 6. Schematic Diagram of the Scanning Mechanism

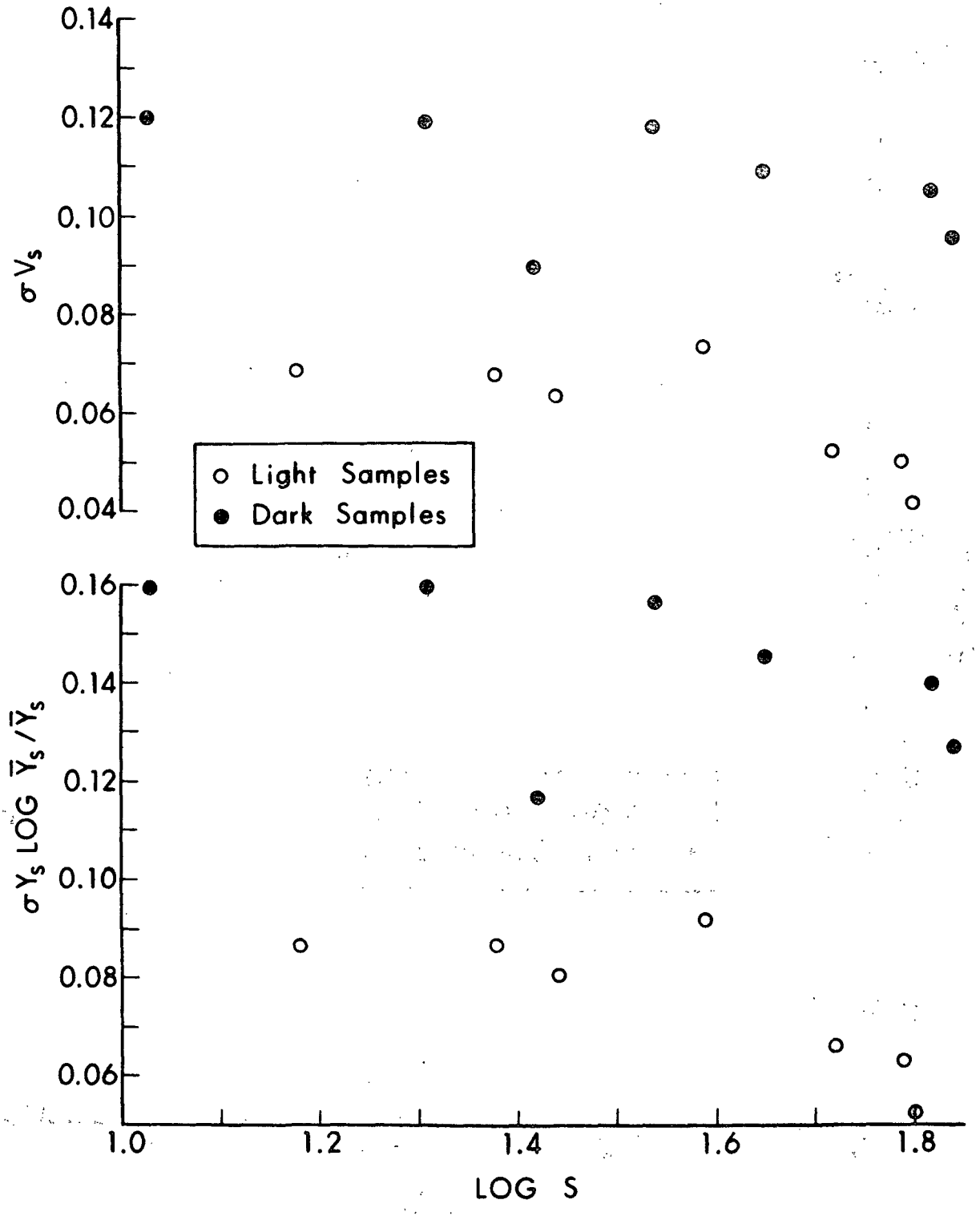

Figure 7. Plot of σV_S and σY_S log $\overline{Y}_S/\overline{Y}_S$ vs. log of Subjective Evenness for Mixed Light and Dark Letterpress Halftone Prints.

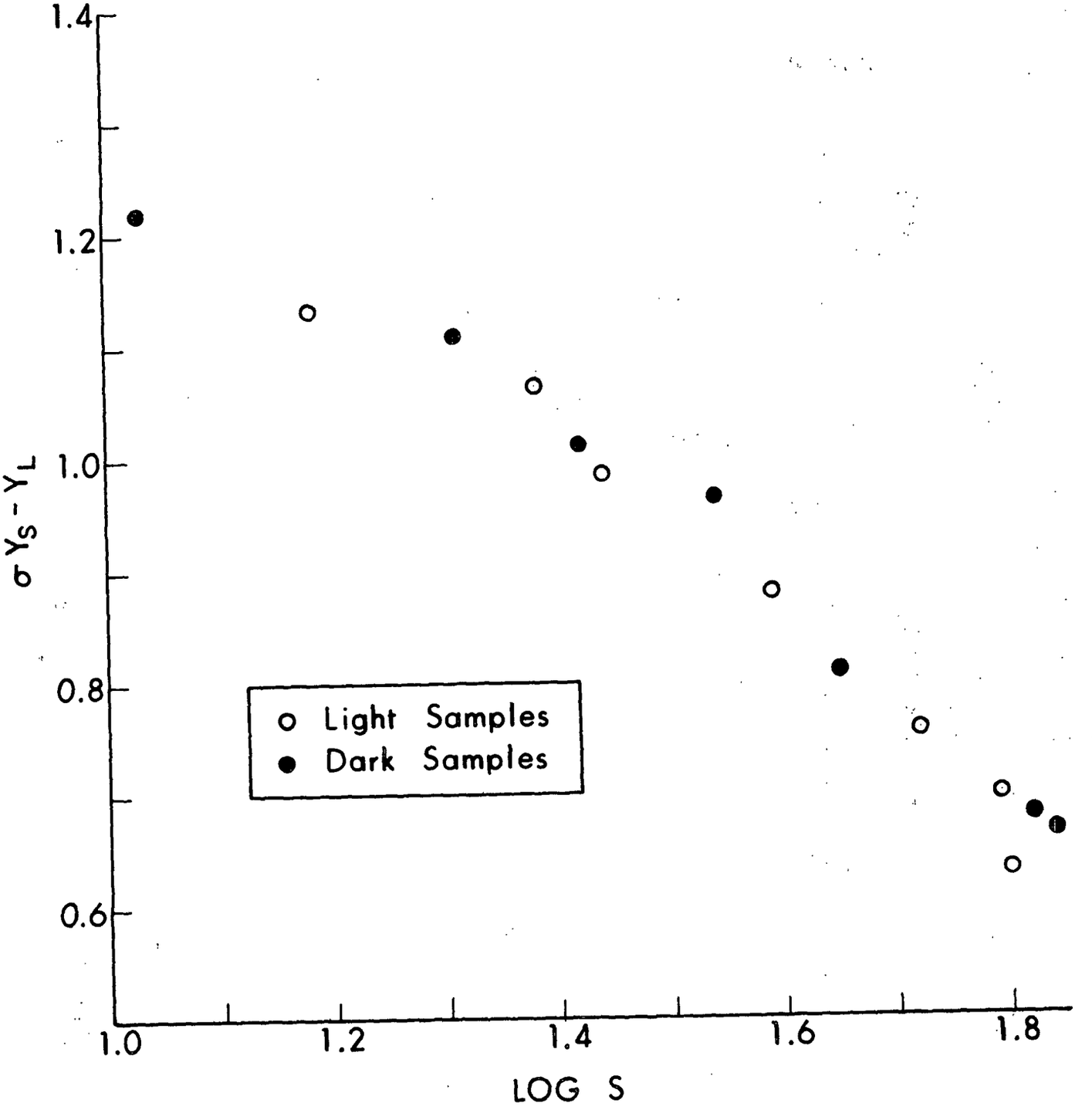

Figure 8. Plot of $\sigma_{Y_S - Y_L}$ vs. log of Subjective Evenness for Mixed Light and Dark Letterpress Halftone Prints.